A New Observation of the Elliot Curve Waveform in Charge Pumping of Poly-Si TFTs

Lei Lu, Mingxiang Wang, *Senior Member, IEEE*, and Man Wong, *Senior Member, IEEE*

***Abstract*—In the charge pumping (CP) measurement of poly-Si thin-film transistors (TFTs), the Elliot curve is found to be irrelevant to the flat-band voltage ($V_{\rm fb}$) and threshold voltage ($V_{\rm th}$) and hence does not follow the traditional MOSFET CP rule. Instead, a new correspondence between the TFT Elliot curve and device key parameters is observed. The critical onset voltages of the CP current are the threshold gate voltages for channel inversion and accumulation, which can be experimentally extracted by capacitance–voltage measurement. They are consistent with the general CP model and reduce to $V_{\rm fb}$ and $V_{\rm th}$ in MOSFETs.**

***Index Terms*—Charge pumping (CP), Elliot curve, poly-Si, thin-film transistors (TFTs).**

I. Introduction

CHARGE pumping (CP) is a standard technique to evaluate the interface trap state density (D_t) in MOSFETs [1]–[3]. When CP currents ($I_{\rm cp}$) are measured against the step increased gate pulse base voltage ($V_{\rm gb}$) with a fixed pulse height ($V_{\rm ph}$), an Elliot curve is obtained [1]. Ideally, its waveform is cap shaped with a central plateau and two steep transition edges at $V_{\rm gb} \approx V_{\rm th} - V_{\rm ph}$ and $V_{\rm fb}$ [see Fig. 1(a)]. The constant $I_{\rm cp}$ is normally used to calculate D_t with its onset V_g's, i.e., $V_{\rm fb}$ and $V_{\rm th}$ as extraction parameters [1]. Moreover, Elliot curves are also used to investigate the device degradation [2]. However, their waveforms in poly-Si thin-film transistors (TFTs) were far from ideal, which previously was ascribed to the fabrication process [4] or some unknown traps [5]. It prevents the clarification of the correspondence between the device characteristics and the Elliot curve. Thus, the traditional MOSFET CP rule was still followed in poly-Si TFTs [4]–[8].

Recently, it was revealed that the geometric effect largely affects the Elliot curve waveforms in poly-Si TFTs. Once it is minimized [10], regular cap-shaped Elliot curves can be reliably obtained. However, the transition edges are irrelevant to $V_{\rm fb}$ or $V_{\rm th}$, indicating the invalidity of the MOSFET rule for TFTs. Moreover, the transition edges are not steep at all. Thus, it is more reasonable that each edge corresponds to two different $V_{\rm gb}$ values at the start and end points, respectively. In this letter, such a correspondence between the Elliot curve and TFT characteristics is first observed. It provides one a better understanding of the Elliot curve in TFTs and a feasible tool for characterizing poly-Si TFTs and their degradation. Moreover, D_t can be more accurately extracted using corrected onset V_g's.

Manuscript received November 16, 2010; accepted December 28, 2010. Date of publication February 22, 2011; date of current version March 23, 2011. This work was supported in part by the National Natural Science Foundation (NNSF) of China under Grant 61076085, by the NNSF of Jiangsu Province of China under Grant BK2009112, and by the State Key Laboratory of ASIC & System under Grant 10KF002. The review of this letter was arranged by Editor A. Nathan.

L. Lu is with the Department of Microelectronics, Soochow University, Suzhou 215006, China, and also with the Department of Electronic and Computer Engineering, Hong Kong University of Science and Technology, Kowloon, Hong Kong.

M. Wang is with the Department of Microelectronics, Soochow University, Suzhou 215006, China (e-mail: Mingxiang_wang@suda.edu.cn).

M. Wong is with the Department of Electronic and Computer Engineering, Hong Kong University of Science and Technology, Kowloon, Hong Kong.

Color versions of one or more of the figures in this letter are available online at http://ieeexplore.ieee.org.

Digital Object Identifier 10.1109/LED.2010.2104311

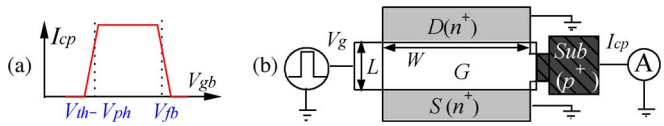

Fig. 1. (a) Correspondence rule for the MOSFET Elliot curve. (b) Planar view of an n-channel poly-Si TFT ($W/L = 30/10\ \mu$m) under CP test.

II. Elliot Curves in Poly-Si TFTs

The planar view of an n-channel poly-Si TFT under CP test is illustrated in Fig. 1(b). For low-temperature (LT) TFTs, poly-Si was formed by the solution-based metal-induced crystallization [11] of a-Si at 630 °C, while for high-temperature (HT) devices, an additional recrystallization was done at 900 °C. V_g pulses are applied with the source (S) and drain (D) grounded, and $I_{\rm cp}$ is measured from p^+-doped substrate side contact. V_g pulse parameters include base/peak voltage $V_{\rm gb}/V_{\rm gp}$ and rising/falling time t_r/t_f.

In Fig. 2, an LT TFT transfer curve at a drain voltage (V_d) of 0.1 V is plotted in semi-log and linear scales. $V_{\rm fb} = 0$ V is estimated as the V_g bias of the minimum drain current (I_d) [12]. $V_{\rm th} = 10$ V is extracted as the intercept of linear extrapolation of the transfer curve. According to the MOSFET CP model [1]–[3], $I_{\rm cp}$ should be obtained when V_g pulses span the hatched transition region between $V_{\rm fb}$ and $V_{\rm th}$. For example, if $I_{\rm cp}$ is measured by using V_g pulses with fixed amplitude $V_{\rm ph} = 22$ V and increasing $V_{\rm gb}$ (e.g., pulses I to V in Fig. 2), $I_{\rm cp}$ arises for the V_g pulses between pulses II ($V_{\rm gp} = V_{\rm th}$) and IV ($V_{\rm gb} = V_{\rm fb}$). When the entire V_g pulse is within the accumulation or strong inversion region, such as pulse I ($V_{\rm gp} = V_{\rm fb}$) or V ($V_{\rm gb} = V_{\rm th}$), no $I_{\rm cp}$ arises. Thus, an ideal Elliot curve is cap shaped, where $V_{\rm fb}$ and $V_{\rm th}$ are critical onset V_g's of the constant $I_{\rm cp}$ [1]–[3]. The dotted line is a measured Elliot curve from the LT TFT by using optimized V_g pulses with $V_{\rm ph} = 22$ V and a large enough t_r/t_f of 1 ms to minimize the geometric effect [10]. However, unlike the MOSFET model, the onset V_g's in TFTs are apparently irrelevant to $V_{\rm fb}$ and $V_{\rm th}$, and the edges of the Elliot curve are not steep at all. Therefore, in poly-Si TFTs, it is more reasonable that each edge corresponds to two different $V_{\rm gb}$ values at the start and end points, respectively.

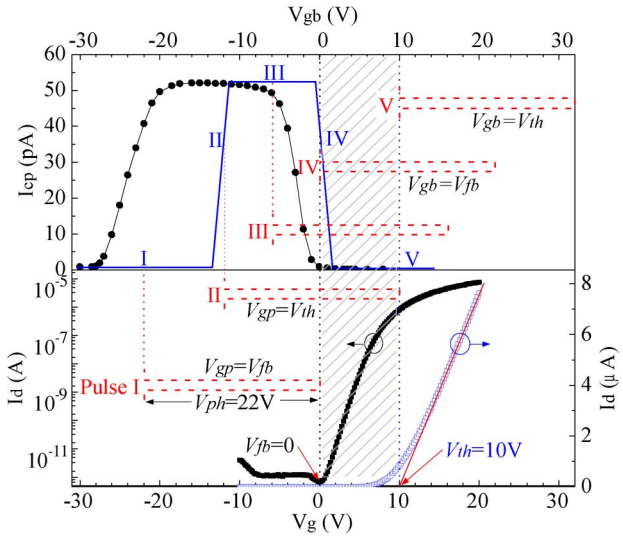

Fig. 2. LT TFT transfer curve at $V_d = 0.1$ V is plotted in linear and semi-log scales, where $V_{\rm fb}$ and $V_{\rm th}$ are extracted. As indicated by the pulses I to V, the MOSFET CP model of the (blue line) Elliot curve corresponds to extracted $V_{\rm fb}$ and $V_{\rm th}$ and is different from the (black solid line) experimental curve of the LT TFTs measured with a $V_{\rm ph}$ of 22 V, a pulse period of 10 ms, a pulse duty ratio of 50%, and a t_r/t_f of 1 ms.

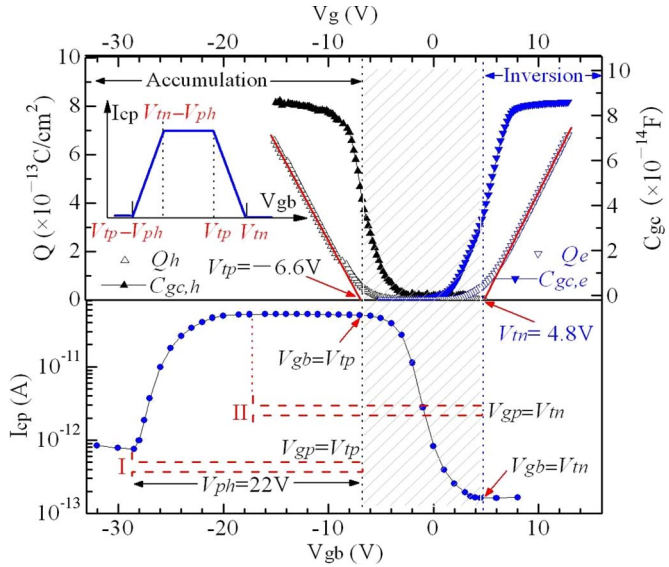

Fig. 3. LT TFT CV curves at $f = 30$ kHz are measured between gate and drain or substrate and used to calculate $Q - V_g$ curves from which $V_{\rm tn}$ and $V_{\rm tp}$ are extracted and correspond to the experimental Elliot curve of Fig. 2 replotted in the semi-log scale, which suggests a new correspondence between the Elliot curve and TFT key parameters in the inset.

III. Observation of the New Correspondence

There is a key difference between poly-Si TFTs and MOSFETs. In MOSFETs, $V_{\rm th}$ is the onset of the channel strong inversion, while in poly-Si TFTs, at $V_g = V_{\rm th}$, not only are the channel grains in strong inversion but also the grain boundary potential barriers are sufficiently suppressed for the carrier to flow over [13]. Therefore, $V_{\rm tn}$ is defined to denote the required V_g for strong inversion in n-channel TFTs, where electron concentration (n_e) becomes reasonably high [13]. In Fig. 3, the gate-to-channel capacitance $(C_{{\rm gc},e})$ of an n-channel LT TFT is measured against V_g. From the CV curve, the sheet density of the inversion electron (Q_e) versus V_g is obtained. $V_{\rm tn}$ is extracted from the intercept of its linear extrapolation [13]. To reasonably compare the CV and CP tests, the same traps should be involved because only fast traps can respond to the measurement signal at a certain f (or t_r/t_f) for the CV (or CP) test due to varied trap emission time [14]. Therefore, a proper f is determined as 30 kHz (or 10 kHz) in LT (or HT) TFTs [14]. The obtained $V_{\rm tn}$ of 3.2 V is much smaller than $V_{\rm th}$, although, in MOSFETs, they are the same. Similarly, $V_{\rm tp}$ is defined as the required V_g where the hole density (n_h) becomes reasonably high. In MOSFETs, $V_{\rm tp}$ equals $V_{\rm fb}$ since the substrate is usually moderately p-doped. In LT TFTs, $V_{\rm tp} = -6.6$ V is extracted by measuring the CV between the gate and the p^+-doped substrate contact (see Fig. 3). It largely differs from $V_{\rm fb}$ too. With $V_{\rm tn}$ and $V_{\rm tp}$ extracted, three V_g regions can be defined: accumulation $(V_g < V_{\rm tp})$, inversion $(V_g > V_{\rm tn})$, and transition $(V_{\rm tp} < V_g < V_{\rm tn})$ regions. Comparing the experimental Elliot curve with $V_{\rm tp}$ and $V_{\rm tn}$ in Fig. 3, a constant $I_{\rm cp}$ is obtained when V_g pulses span the hatched transition region. Moreover, when the entire pulse is within the accumulation or inversion region, $I_{\rm cp}$ decays to a minimum level as shown by the log-scale plot. A new correspondence for the Elliot curve is observed. The start and end points of the rising (or falling) edge of the Elliot curves

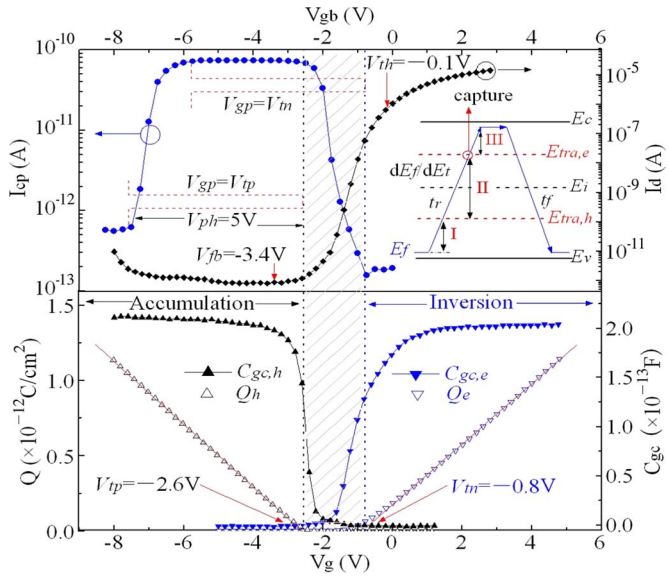

Fig. 4. HT TFT Elliot curve is measured with a $V_{\rm ph}$ of 5 V, a pulse period of 10 ms, a pulse duty ratio of 50%, and a t_r/t_f of 1 ms. Its onset V_g's are observed to be $V_{\rm tp}$ and $V_{\rm tn}$ extracted from CV curves at $f = 10$ kHz, rather than $V_{\rm fb}$ and $V_{\rm th}$ obtained from transfer curves at $V_d = 0.1$ V.

in poly-Si TFTs should correspond to $V_{\rm gb} = V_{\rm tp} - V_{\rm ph}$ and $V_{\rm tn} - V_{\rm ph}$ (or $V_{\rm gb} = V_{\rm tp}$ and $V_{\rm tn}$), while the onset V_g's of the constant $I_{\rm cp}$ are $V_{\rm tp}$ and $V_{\rm tn}$. In Fig. 4, the same correspondence is observed in HT TFTs, although the discrepancy between $V_{\rm fb}/V_{\rm th}$ and $V_{\rm tp}/V_{\rm tn}$ in HT TFTs is notably smaller than that in LT TFTs since the fabrication process strongly affects the TFT quality and HT recrystallization produces much better poly-Si crystallinity. The same correspondence is also observed at other f's for the CV and respective t_r/t_f's for the CP test.

Comparing Elliot curves in MOSFETs and TFTs, the onset V_g's of the constant $I_{\rm cp}$ largely differ. It can be understood from the CP model [1]–[3]. In the inset in Fig. 4, during t_r, the

surface potential (E_f) is swept at a certain rate, $\mathrm{d}E_f/\mathrm{d}t$ ($\dot{E}_f$). In order to keep the trap occupation in equilibrium with the E_f sweep, holes trapped in donorlike traps will be emitted to the valence band (E_v) at a rate

$$(\dot{E}_t)_h = kTv_{\mathrm{th}}\sigma n_h \tag{1}$$

where E_t, k, T, σ, and v_{th} are the trap quasi-Fermi level, Boltzmann constant, temperature, capture cross section, and thermal velocity, respectively [3]. The sweeping E_f drives TFTs from accumulation to inversion. n_h is initially high enough; thus, $(\dot{E}_t)_h = \dot{E}_f$ so that the hole emission is in a steady state (region I). Subsequently, with n_h reduced and $(\dot{E}_t)_h < \dot{E}_f$, nonsteady-state emission occurs (region II). It continues until n_e becomes high enough so that $(\dot{E}_t)_e > \dot{E}_f$ and the steady-state electron capture occurs (region III). Transition trap levels $E_{\mathrm{tra},h}$ and $E_{\mathrm{tra},e}$ are defined to separate regions I, II, and III by equating $\dot{E}_f$ with $(\dot{E}_t)_h$ or $(\dot{E}_t)_e$ [1]–[3]. The remaining holes between the two levels after the nonsteady-state emission will be recombined with the captured electrons from the conduction band (E_c) and contribute to I_{cp}. A similar process occurs also during t_f. Thus, the onsets of I_{cp} are V_g positions corresponding to $E_{\mathrm{tra},h}$ and $E_{\mathrm{tra},e}$, respectively [1]–[3]. According to (1), obviously, only when n_e or n_h becomes reasonably high can $(\dot{E}_t)_e$ or $(\dot{E}_t)_h$ meet $\dot{E}_f$ [3]. That is why the onset V_g's of the constant I_{cp} should be V_{tp} and V_{tn}. They are more fundamental and reduce to V_{fb} and V_{th} in MOSFETs. Both experimental evidences and theoretical analysis demonstrate the applicability of V_{tp} and V_{tn} as onset V_g's of the constant I_{cp}. Thus, D_t extraction equations for TFTs [10] should be modified by revising the onset V_g's as V_{tp} and V_{tn}. Since the analysis is based on general CP models [1]–[3], we expect that such a correspondence should be also applicable to other field-effect devices, such as SiC MOSFETs [8].

On the other hand, the transition edges of TFT Elliot curves are much broader than those in MOSFETs. It may derive from two aspects. First, the poly-Si TFT channel consists of many grains. Their V_{tp} and V_{tn} depend on the grain size and D_t and vary in several volts [15]. Generally, the mentioned device V_{tp} (or V_{tn}) is associated with the accumulation (or inversion) of the entire channel, i.e., close to the maximum V_{tp} (or V_{tn}) among all grains. Each grain provides an "Elliot curve," the sum of which is the measured overall Elliot curve. Thus, transition edges may derive from those grains with smaller V_{tp} and V_{tn}, while the constant I_{cp} originates from all grains. Hence, the onset V_g's are device V_{tp} and V_{tn}. Therefore, the large variation of V_{tp} and V_{tn} among all grains can contribute to the broad transition edges of the TFT Elliot curve. Second, the effects that broaden MOSFET transition edges [1] may still work in TFTs, e.g., the lateral variation of V_{th} and V_{fb} near the source and drain junctions [1]. Both aspects should contribute to the gradual transition edges of the TFT Elliot curves.

IV. Conclusion

Unlike in MOSFETs, the onset V_g's of the constant I_{cp} in poly-Si TFTs are not the V_{fb} and V_{th} derived from the transfer curve but are the V_{tp} and V_{tn} extracted from the CV curve. They are consistent with the CP model [3] and reduce to V_{fb} and V_{th} in MOSFETs. Moreover, the variation of V_{tp} and V_{tn} among channel grains and the effects broadening MOSFET transition edges [1] should contribute to the broad transition edges of the TFT Elliot curves.

References

[1] G. Groeseneken, H. E. Maes, N. Beltran, and R. F. De Keersmaecker, "A reliable approach to charge-pumping measurements in MOS transistors," *IEEE Trans. Electron Devices*, vol. ED-31, no. 31, pp. 42–53, Jan. 1984.

[2] P. Heremans, J. Witters, G. Groeseneken, and H. E. Maes, "Analysis of the charge pumping technique and its application for the evaluation of MOSFET degradation," *IEEE Trans. Electron Devices*, vol. 36, no. 7, pp. 1318–1335, Jul. 1989.

[3] D. Bauza, "A general and reliable model for charge pumping—Part I: Model and basic charge-pumping mechanisms," *IEEE Trans. Electron Devices*, vol. 56, no. 1, pp. 70–77, Jan. 2009.

[4] N. S. Saks, S. Batra, and M. Manning, "Charge pumping in thin film transistors," *Microelectron. Eng.*, vol. 28, no. 1–4, pp. 379–382, Jun. 1995.

[5] M. Koyanagi, I. W. Wu, A. G. Lewis, M. Fuse, and R. Bruce, "Evaluation of polycrystalline silicon thin film transistors with the charge pumping technique," in *IEDM Tech. Dig.*, 1990, pp. 863–866.

[6] C. Y. Chen, M. W. Ma, W. C. Chen, H. Y. Lin, K. L. Yeh, S. D. Wang, and T. F. Lei, "Analysis of negative bias temperature instability in body-tied low-temperature polycrystalline silicon thin-film transistors," *IEEE Electron Device Lett.*, vol. 29, no. 2, pp. 165–167, Feb. 2008.

[7] T. Yoshida, Y. Ebiko, M. Takei, N. Sasaki, and T. Tsuchiya, "Grain-boundary related hot carrier degradation mechanism in low-temperature polycrystalline silicon thin-film transistors," *Jpn J. Appl. Phys.*, vol. 42, no. 4B, pp. 1999–2003, 2003.

[8] D. Okamoto, H. Yano, T. Hatayama, Y. Uraoka, and T. Fuyuki, "Analysis of anomalous charge pumping characteristics on 4H-SiC MOSFETs," *IEEE Trans. Electron Devices*, vol. 55, no. 8, pp. 2013–2020, Aug. 2008.

[9] G. Van den Bosch, G. Groeseneken, and H. E. Maes, "On the geometric component of charge pumping current in MOSFETs," *IEEE Electron Device Lett.*, vol. 14, no. 3, pp. 107–109, Mar. 1993.

[10] L. Lu, M. Wang, and M. Wong, "Geometric effect elimination and reliable trap state density extraction in charge pumping of polysilicon thin-film transistors," *IEEE Electron Device Lett.*, vol. 30, no. 5, pp. 517–519, May 2009.

[11] B. Zhang, Z. Meng, S. Zhao, M. Wong, and H. S. Kwok, "Polysilicon thin film-transistors with uniform and reliable performance using solution-based metal-induced crystallization," *IEEE Trans. Electron Devices*, vol. 54, no. 5, pp. 1244–1248, May 2007.

[12] C. Y. Chen, J. W. Lee, S. D. Wang, M. S. Shieh, P. H. Lee, W. C. Chen, H. Y. Lin, K. L. Yeh, and T. F. Lei, "Negative bias temperature instability in low-temperature polycrystalline silicon thin-film transistors," *IEEE Trans. Electron Devices*, vol. 53, no. 12, pp. 2993–3000, Dec. 2006.

[13] H. Hao, M. Wang, B. Zhang, X. Shi, and M. Wong, "A comprehensive analytical on-current model for polycrystalline silicon thin film transistors based on effective channel mobility," *J. Appl. Phys.*, vol. 103, no. 9, pp. 094513-1–094513-10, May 2008.

[14] M. D. Jacunski, M. S. Shur, and M. Hack, "Threshold voltage, field effect mobility, and gate-to-channel capacitance in polysilicon TFTs," *IEEE Trans. Electron Devices*, vol. 43, no. 9, pp. 1433–1440, Sep. 1996.

[15] C. A. Dimitriadis and D. H. Tassis, "On the threshold voltage and channel conductance of polycrystalline silicon thin-film transistors," *J. Appl. Phys.*, vol. 79, no. 8, pp. 4431–4437, Apr. 1996.